

Unifying Speech Editing Detection and Content Localization via Prior-Enhanced Audio LLMs

Jun Xue ^{*1} Yi Chai ^{*1} Yanzhen Ren ¹ Jinshen He ² Zhiqiang Tang ³ Zhuolin Yi ¹ Yihuan Huang ¹
Yuankun Xie ⁴ Yujie Chen ⁵

Abstract

Speech editing achieves semantic inversion by performing fine-grained segment-level manipulation on original utterances, while preserving global perceptual naturalness. Existing detection studies mainly focus on manually edited speech with explicit splicing artifacts, and therefore struggle to cope with emerging end-to-end neural speech editing techniques that generate seamless acoustic transitions. To address this challenge, we first construct a large-scale bilingual dataset, *AiEdit*, which leverages large language models to drive precise semantic tampering logic and employs multiple advanced neural speech editing methods for data synthesis, thereby filling the gap of high-quality speech editing datasets. Building upon this foundation, we propose *PELM* (Prior-Enhanced Audio Large Language Model), the first large-model framework that unifies speech editing detection and content localization by formulating them as an audio question answering task. To mitigate the inherent *forgery bias* and *semantic-priority bias* observed in existing audio large models, *PELM* incorporates word-level probability priors to provide explicit acoustic cues, and further designs a centroid-aggregation-based acoustic consistency perception loss to explicitly enforce the modeling of subtle local distribution anomalies. Extensive experimental results demonstrate that *PELM* significantly outperforms state-of-the-art methods on both the *HumanEdit* and *AiEdit* datasets, achieving equal error rates (EER) of 0.57% and 9.28% (localization), respectively.

¹Key Laboratory of Aerospace Information Security and Trusted Computing, Ministry of Education; School of Cyber Science and Engineering, Wuhan University, Wuhan, China

²Independent Researcher ³School of Computer Science and Technology, Anhui University, Hefei, China ⁴Communication University of China, Beijing, China ⁵Beihang University, Beijing, China.

Correspondence to: Yanzhen Ren <renyz@whu.edu.cn>.

Preprint. January 30, 2026.

1. Introduction

With the rapid advancement of large-scale data and deep learning technologies, high-fidelity audio generation has become increasingly prevalent. While significantly improving production efficiency, it also poses serious threats to personal privacy and societal security. Audio deepfake threats can be broadly categorized into fully synthetic forgeries and segment-level speech editing. The former generates complete utterances using Text-to-Speech (TTS) (Chen et al., 2025) or Voice Conversion (VC) (Yao et al., 2025) techniques, thereby altering the global signal distribution. In contrast, the latter performs addition, deletion, or modification operations on only specific segments, achieving semantic reversal through extremely short information manipulations (e.g., negations or key entities) while preserving most of the original speaker’s voice characteristics and background context. Such localized manipulations are highly covert and deceptive, exhibiting substantial destructive potential in scenarios such as fake news dissemination, public opinion manipulation, and financial fraud.

Existing speech editing techniques can be broadly categorized into two paradigms. The first paradigm is traditional rule-based acoustic editing (Zhang et al., 2023), whose pipeline typically consists of voice activity detection (VAD)-based segmentation, segment synthesis, and manual splicing. This process is highly prone to cumulative errors, often leaving prominent acoustic boundary artifacts between the forged regions and the original background, which causes conventional detection models to rely heavily on capturing such low-level signal traces. The second paradigm, which poses a more severe threat, is end-to-end neural speech editing (Zhang et al., 2025). It leverages advanced models to perform localized editing guided by semantic instructions, generating edited segments that are highly consistent with the surrounding prosody and context. Such end-to-end editing not only eliminates splicing artifacts but also exhibits extremely high semantic controllability and imperceptibility. Notably, although these models enforce strong constraints to preserve the integrity of non-edited regions, the output audio still typically undergoes reconstruction via neural audio representations (e.g., neural codecs). The reconstruction

artifacts introduced in this process are acoustically highly similar to the compression distortions (Yamagishi et al., 2021) encountered in real-world communication scenarios, thereby shifting the detection challenge from identifying explicit reconstruction traces to precisely distinguishing semantic tampering from subtle generative artifacts.

To counter these emerging threats, current research on speech editing detection (SED) has predominantly focused on segment-based or boundary-aware paradigms. For instance, Martín-Doñas et al. (Martín-Doñas & Álvarez, 2022) employed a two-stage framework combining Wav2Vec features with BiLSTM for segment clustering, while TDL (Xie et al., 2024) introduced an embedding similarity module to distinguish the feature distributions of bona fide and forged frames. To move beyond purely segment-level analysis, CFPFR (Wu et al., 2024) and BAM (Zhong et al., 2024) integrated boundary-aware mechanisms designed to locate forgery transitions by capturing manual splicing artifacts or utilizing coarse-to-fine proposal networks. However, these methods exhibit significant limitations: they are primarily optimized for the acoustic discontinuities and low-level signal artifacts inherent in traditional manually edited datasets. Consequently, they struggle to detect end-to-end edited speech, which maintains high acoustic consistency without discernible splicing traces. Furthermore, although the related dataset (Zhang et al., 2025) has been proposed, its partial public access has hindered in-depth exploration.

To address the above challenges, this paper first constructs a high-quality dataset, namely AiEdit. This dataset leverages large language models (LLMs) to drive precise semantic modifications and integrates multiple state-of-the-art neural speech editing technologies to generate samples. Furthermore, we propose the Prior-Enhanced Audio Large Language Model (PELM) framework, which is the first large model specifically designed for speech editing detection and content localization. To address the prevalent *forgery bias* (Röttger et al., 2024) (i.e., a tendency to over-predict forgery) and *semantic-priority bias* (Wang et al., 2025b) (i.e., excessive focus on semantic content while neglecting low-level acoustic signals) observed in existing audio LLMs, PELM incorporates a word-level probabilistic prior and an acoustic consistency-aware loss for effective mitigation. Specifically, the prior is obtained by aggregating frame-level probabilities generated by a frame-level detector according to word boundaries, thereby providing explicit acoustic cues for Audio LLMs. Meanwhile, the acoustic consistency-aware loss models the distribution of feature centroid distances, forcing the model to capture subtle acoustic discontinuities by minimizing the centroid deviation of bona fide speech and maximizing the dispersion of Top-K anomalous frames in edited speech during training, thus effectively suppressing semantic drift.

The main contributions are summarized as follows:

- We construct the first large-scale, high-quality AiEdit dataset: by introducing LLMs as a semantic engine and integrating multiple advanced neural speech editing technologies, AiEdit enables precise addition, deletion, and modification operations on textual content, filling the gap of high-quality speech edited data benchmarks. The dataset¹ is available.
- We propose the first large-model-based unified framework for speech editing detection and content localization, namely PELM: by incorporating a word-level probabilistic prior and an acoustic consistency-aware loss, PELM significantly mitigates the forgery bias and semantic-priority bias of Audio LLMs.
- We conduct extensive performance evaluations and ablation studies: experimental results demonstrate that PELM consistently outperforms existing state-of-the-art methods on both the HumanEdit and AiEdit.

2. Motivation

2.1. Threat Methods

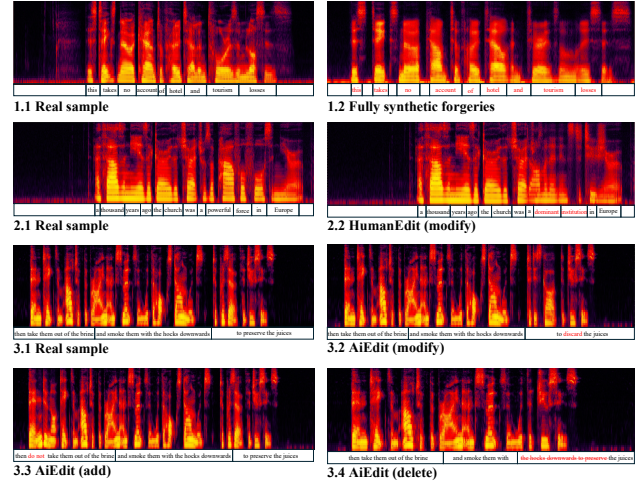


Figure 1. Spectrogram comparison across different editing samples.

Fully Synthetic Forgery: Early research on fake speech detection primarily focused on fully synthetic attacks, which aim to spoof entire utterances to compromise automatic speaker verification (ASV) systems, as exemplified by the ASVspoof (Todisco et al., 2019; Yamagishi et al., 2021) and ADD (Yi et al., 2023b) challenge series. As illustrated in Figs. 1 (1.1 and 1.2), although the generated speech exhibits high perceptual quality, its target speaking style undergoes evident global transformation. Compared with the compact

¹<https://huggingface.co/datasets/JunXueTech/AiEdit>

Table 1. Statistical comparison and attribute overview of partial spoofing datasets. Note that “-” indicates the information is not publicly available or applicable.

Dataset	Ref.	Year	Datasource	Language	Operations	Access	#Utterances		MOS
							Real	Fake	
PartialSpoof	(Zhang et al., 2023)	2021	ASVspoof 2019 LA	English	modify	Public	12,483	108,978	3.41 ± 0.21
HAD	(Yi et al., 2021)	2021	AISHELL-3	Chinese	modify	Public	53,612	53,612	3.43 ± 0.17
ADD2022Track2	(Yi et al., 2022)	2022	AISHELL-3	Chinese	modify	Public	5,319	1,052	-
Psynd	(Zhang & Sim, 2022)	2022	LibriTTS	English	modify	Restrict	-	-	-
LAV-DF	(Cai et al., 2022)	2022	Voxceleb2	English	modify	Public	36,431	99,873	-
ADD2023Track2	(Yi et al., 2023a)	2023	AISHELL-3	Chinese	modify	Public	55,467	63,831	-
PartialEdit	(Zhang et al., 2025)	2025	Voxceleb2	English	modify	Partially Public	-	43,358	3.41 ± 0.21
LlamaPartialSpoof	(Luong et al., 2025)	2025	LibriTTS	English	modify	Public	10,573	32,194	-
AiEdit	Ours	2026	Libriheavy/Chineselp	Chinese/English	add/delete/modify	Public	7,760	51,794	3.77 ± 0.36

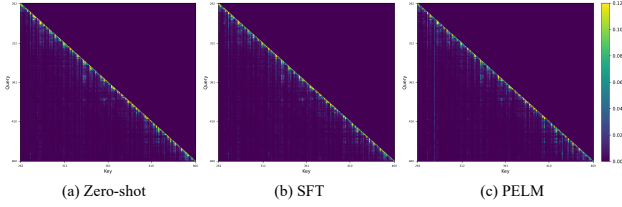


Figure 2. Self-attention heatmaps over the audio token region in the last Transformer layer.

and coherent prosody of bona fide samples, synthetic speech often sounds mechanical, with overly deliberate and complete articulation, leading to unnatural listening impressions.

HumanEdit: To preserve most characteristics of the original speaker while manipulating local semantics, researchers have proposed partial forgery based on the “cut-and-paste” paradigm, with PartialSpoof (Zhang et al., 2023) as a representative work. This approach synthesizes local segments via TTS or VC and then splices them into bona fide speech using heuristic rules. As shown in Figs. 1 (2.1 and 2.2), this method suffers from evident limitations. On the one hand, naive splicing operations introduce conspicuous acoustic artifacts at editing boundaries; on the other hand, since random timestamp truncation is commonly adopted, the edited utterances often exhibit grammatical errors or logical discontinuities. **AiEdit:** To overcome the drawbacks of human editing, end-to-end neural speech editing models (Yan et al., 2025; Jiang et al., 2023) have been developed to enable highly controllable and multi-type editing operations, including modification, addition, and deletion. Under contextual constraints, these models can generate speech segments that are highly consistent with the original audio in terms of prosody and speaking style. As illustrated in Figs. 1 (3.1–3.4), AiEdit not only ensures fluent semantic logic but also eliminates the artificial artifacts introduced by traditional splicing, achieving seamless fusion between the edited regions and the background context.

Summary: Fully synthetic forgery mainly aims to impersonate the speaker to deceive authentication systems. In contrast, in malicious dissemination and misinformation fraud scenarios, semantic manipulation achieved through minimal

modifications, namely speech editing, constitutes a more threatening and covert attack paradigm. Therefore, this work focuses on defending against more advanced speech editing attacks.

2.2. Audio LLMs

In recent years, Audio LLMs have demonstrated great potential in fully synthetic speech detection (Gu et al., 2025). However, compared with synthetic attacks that alter the global signal distribution, speech editing and its content localization require the model to conduct extremely fine-grained acoustic consistency analysis on local signal regions, which poses dual challenges to existing Audio LLMs:

1) Forgery Bias: Audio LLMs are highly susceptible to exhibiting excessive sensitivity in the form of forgery bias. This phenomenon is closely related to the overly conservative decision boundaries (Röttger et al., 2024) formed during the reinforcement learning from human feedback (RLHF) stage, where the model tends to misclassify low-quality bona fide signals as synthetic in order to avoid potential risks. To address this issue, we introduce a word-level probabilistic prior to explicitly calibrate the model’s reasoning boundaries using external acoustic evidence.

2) Semantic Priority: During fine-tuning, existing Audio LLMs often overemphasize instruction alignment and semantic (Wang et al., 2025b) coherence while neglecting low-level acoustic details, leading to a semantic-priority bias. As a result, the model struggles to capture the extremely smooth acoustic transitions produced by advanced neural speech editing techniques. To this end, we design an acoustic consistency-aware loss that enforces clustering constraints in the feature space, compelling the model to attend to local acoustic anomalies and thereby mitigating semantic drift.

The self-attention heatmap visualization over the audio regions (see Fig. 2) provides strong empirical support for the above motivations. Under the Zero-shot or conventional SFT settings, the model exhibits relatively diffuse attention distributions, failing to effectively focus on localized tamper-

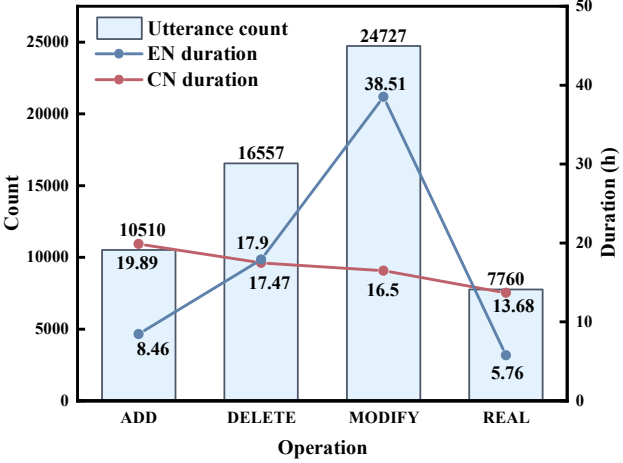


Figure 3. Statistical overview of the dataset composition. The bar chart (left axis) displays the total sample count for each operation type (Add, Delete, Modify) and real speech. The line plot (right axis) illustrates the total audio duration in hours for the English (blue) and Chinese (red) subsets.

ing regions; whereas after incorporating the proposed prior and consistency constraints (PELM), the response intensity of the model in critical anomalous regions is significantly enhanced.

3. The AiEdit Dataset

3.1. Dataset Construction

Existing open-source datasets predominantly follow traditional fabrication paradigms that rely on manual selection of editing segments and simplistic concatenation (e.g., inserting TTS-generated segments). Such approaches suffer from inherent limitations: on the one hand, unstructured editing often fails to achieve targeted semantic manipulations with explicit deceptive intent; on the other hand, crude splicing operations inevitably introduce unnatural acoustic discontinuities at the boundaries between forged segments and the original background, making them easily detectable by methods that exploit low-level signal artifacts. To fill the gap of high-quality speech editing data, we construct a large-scale, bilingual speech editing benchmark that covers a diverse range of representative neural speech editing models.

The dataset construction follows a three-stage pipeline, including LLM-driven text editing, multi-type speech editing generation, and post-processing. In the first stage, we select Libriheavy (Kang et al., 2024) and ChineseLips (Zhao et al., 2025) as the English and Chinese source corpora, respectively, and leverage the large language model Qwen3-max to generate target texts via controllable insertion, deletion, and modification operations. Subsequently, in the speech editing stage, to prevent detection models from overfitting

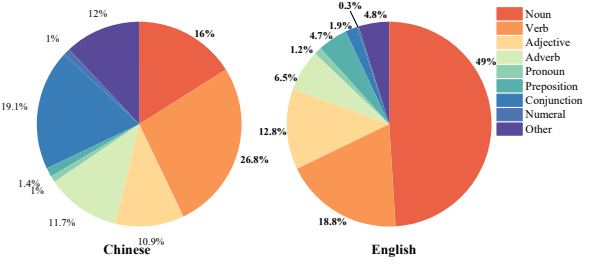


Figure 4. Distribution of Part-of-Speech (POS) tags for edited words. The pie charts illustrate the proportion of different syntactic categories targeted for editing in the Chinese (left) and English (right) subsets of our dataset.

to specific forgery artifacts, we introduce three representative editing paradigms: (1) end-to-end reconstruction models (e.g., SSR (Wang et al., 2025a) and VoiceCraft (Peng et al., 2024)), which directly generate continuous and imperceptible local tampering segments based on textual differences; (2) region-aware inpainting models represented by FluentSpeech (Jiang et al., 2023), supplemented with a dedicated alignment matching algorithm to resolve index offset issues caused by punctuation, thereby enabling precise region-level supervision; and (3) the instruction-driven large-model-based editing framework Ming-UniAudio (Yan et al., 2025), which performs instruction-guided speech editing using audio LLMs. In the post-processing stage, all audio samples are resampled to 16 kHz and saved in WAV format.

3.2. Dataset Statistics

As indicated by the data in Table 1, distinct from previous construction methods that rely on fixed templates or random replacements, AiEdit is the first bilingual dataset capable of uniformly executing three fine-grained operations: addition, deletion, and modification. Our dataset not only expands the dimensions of operation but also achieves significant improvements in speech quality, demonstrating its ability to simulate more complex attack scenarios while maintaining high fidelity.

Figure 3 presents a detailed statistical overview of the dataset. Regarding sample composition, the dataset exhibits a rational distribution gradient: since the modification operation is the most stealthy and prevalent in real world tampering, it accounts for the largest volume of samples. This distribution ensures sufficient training data for primary attack types while also accounting for long-tail operation types.

To validate the depth of semantic editing, we further analyze the linguistic characteristics of the tampered regions. As illustrated in Figure 4, by employing a Large Language Model as the semantic editing engine, AiEdit generates

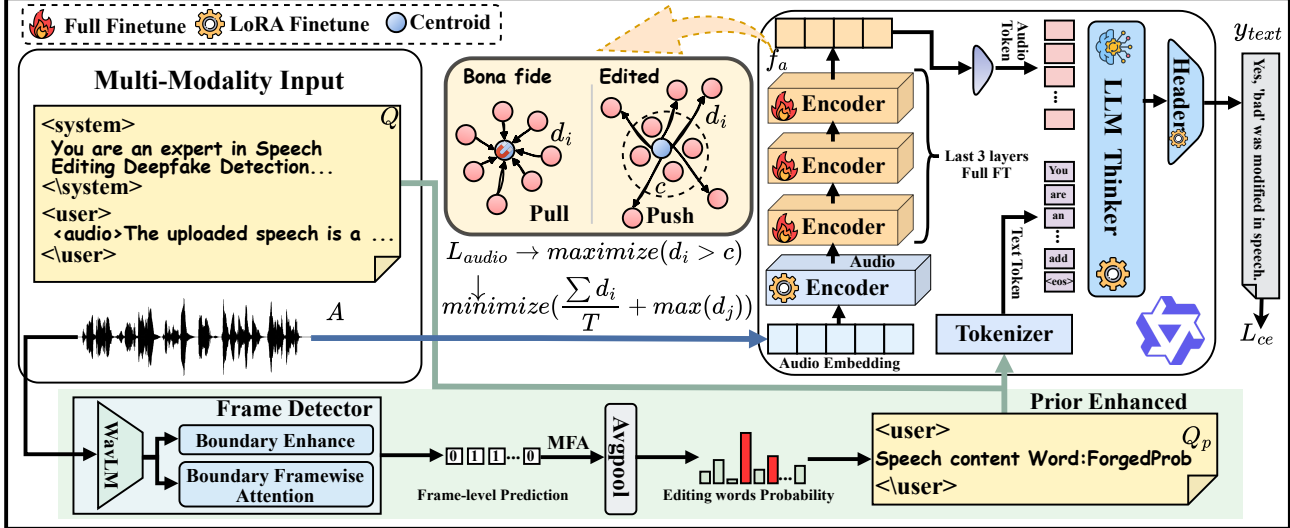


Figure 5. Overview of the PELM architecture, including prior-enhanced multi-modality input construction, audio LLM-based reasoning, and centroid clustering-based training objective.

text tampering schemes covering diverse parts of speech, including nouns, verbs, adjectives, and conjunctions, via context-aware reasoning. Specifically, different languages exhibit distinct editing preferences: in the English subset, nouns are dominant, accounting for 49%, followed by verbs (18.8%) and adjectives (12.8%), which aligns with the structural emphasis on noun phrases in English. Conversely, the distribution within the Chinese subset is more balanced, with verbs occupying the highest proportion at 26.8%, followed closely by nouns (16%) and adverbs (11.7%). This Part-of-Speech distribution, grounded in authentic linguistic patterns, demonstrates that we have maximized the linguistic diversity of forgery patterns while ensuring the semantic coherence of the edited sentences. More details of the dataset are provided in Appendix A.

4. Method

4.1. Task Formulation

To fully leverage the reasoning and generation capabilities of Large Language Models, PELM reformulates speech editing detection and localization as a structured Audio Question Answering (AQA) task. Given an audio segment A , a natural language instruction prompt Q is introduced to guide detection and content localization. To incorporate external acoustic evidence and constrain the reasoning boundaries of the large model, we further inject a structured word-level probabilistic prior prompt Q_p , derived from a frame-level detector. The final response y is generated by jointly conditioning on A , Q , and Q_p :

$$y = M(A, Q, Q_p), \quad (1)$$

where M denotes the PELM model.

To enable standardized parsing and evaluation, strict output format constraints are imposed. For bona fide inputs, the model outputs a fixed declaration: “No evidence of speech editing was detected.”; otherwise, the output must follow the template: “Yes, \langle exact words \rangle was \langle Type \rangle in the speech.”, where \langle Type $\rangle \in \{\text{added, deleted, modified}\}$ specifies the editing operation.

4.2. Prior-Enhanced Fine-tuning

The overall architecture of PELM is illustrated in Fig. 5. Given an audio segment A and its corresponding textual instruction Q , the model first processes A using a pre-trained frame-level detector D to extract frame-wise probabilities, which are then aggregated over word boundaries to obtain a word-level editing probability sequence p . Subsequently, PELM encodes this probability sequence into a structured prior prompt Q_p , explicitly injecting low-level acoustic anomaly information into the large language model. Finally, A , Q , and Q_p are jointly fed into the audio LLM M , which generates a natural language response y , thereby achieving detection and content localization of the edited segments. The training objective aims to maximize the consistency between the generated text and the ground-truth labels, which is implemented via the standard Cross-Entropy Loss:

$$\mathcal{L}_{ce} = -\frac{1}{T} \sum_{t=1}^T \log P(y_t | y_{<t}, A, Q, Q_p) \quad (2)$$

where T denotes the length of the target sequence.

4.3. Acoustic Consistency Aware Loss

To overcome potential semantic drift in Large Language Models when processing audio signals and to enforce the

Table 2. Model Performance Comparison on HumanEdit and AiEdit, and their average (Pool). Best results are **bolded** and second-best results are underlined.

Model	HumanEdit						AiEdit						Pool					
	Detection			Localization			Detection			Localization			Detection			Localization		
	Acc↑	F1↑	EER↓	Acc↑	F1↑	EER↓	Acc↑	F1↑	EER↓	Acc↑	F1↑	EER↓	Acc↑	F1↑	EER↓	Acc↑	F1↑	EER↓
TDL (Xie et al., 2024)	96.25	98.06	14.69	89.34	89.57	10.68	34.95	43.86	49.95	91.02	95.77	35.05	65.60	70.96	32.32	90.18	92.67	22.87
CFPRF (Wu et al., 2024)	97.69	98.71	5.81	86.44	89.54	15.64	65.54	74.89	31.44	90.91	95.16	34.33	81.62	86.80	18.63	88.68	92.35	24.49
AGO (Zeng et al., 2025)	97.76	98.75	4.17	85.78	89.24	15.44	44.93	35.48	28.03	93.50	96.62	27.65	71.35	67.12	16.10	89.64	92.93	21.55
BAM (Zhong et al., 2024)	99.56	<u>99.76</u>	<u>0.63</u>	<u>95.91</u>	<u>96.03</u>	<u>3.78</u>	<u>78.48</u>	<u>85.87</u>	<u>11.66</u>	<u>95.48</u>	97.59	<u>15.89</u>	<u>97.96</u>	<u>92.82</u>	<u>6.15</u>	<u>96.05</u>	<u>96.81</u>	<u>9.84</u>
PELM (Ours)	99.62	<u>99.78</u>	<u>0.55</u>	<u>94.31</u>	<u>99.70</u>	<u>0.57</u>	<u>95.2</u>	<u>97.19</u>	<u>8.37</u>	<u>91.77</u>	<u>97.29</u>	<u>9.28</u>	<u>98.46</u>	<u>98.46</u>	<u>4.46</u>	98.46	<u>98.45</u>	<u>4.93</u>

audio encoder to capture intrinsic differences in feature-space distributions between bona fide and edited speech, we propose a centroid clustering based acoustic consistency-aware loss (\mathcal{L}_{audio}). The key intuition is that the acoustic features of bona fide speech should exhibit high temporal distributional consistency, whereas partially edited speech inevitably contains anomalous frames deviating from the overall distribution.

Specifically, we extract the audio feature sequence $f_a \in \mathbb{R}^{L \times d}$ from the last layer of the audio encoder, where L denotes the number of frames and d the feature dimension. The feature centroid is computed as

$$c = \frac{1}{L} \sum_{i=1}^L f_a^i, \quad (3)$$

and the cosine distance d_i between each frame feature f_a^i and the centroid c is used to measure acoustic deviation.

Based on the audio labels, we design an asymmetric optimization objective:

$$\mathcal{L}_{audio} = \begin{cases} \frac{1}{L} \sum_{i=1}^L d_i + \max(d), & A \in \mathcal{B}, \\ \frac{1}{|S_{topk}|} \sum_{i \in S_{topk}} \text{ReLU}(\text{margin} - d_i), & A \in \mathcal{E}, \end{cases} \quad (4)$$

where \mathcal{B} and \mathcal{E} denote the sets of bona fide and edited speech samples, respectively, and S_{topk} represents the set of the top- $K\%$ frames with the largest deviations.

For bona fide audio, we impose a *cohesion constraint* to enforce all frame features to be tightly clustered around the centroid, optimizing both global compactness and worst-case deviation. Conversely, for edited audio, we impose a *dispersion constraint*, which enlarges the separation between the centroid and anomalous frames to amplify subtle local acoustic discrepancies.

Finally, the overall training objective is formulated as:

$$\mathcal{L}_{total} = \mathcal{L}_{ce} + \lambda \cdot \mathcal{L}_{audio}, \quad (5)$$

where λ is a balancing coefficient.

5. Experiments

5.1. Experimental Setting

In the main experimental phase, we first reproduced several representative state-of-the-art (SOTA) methods on the HumanEdit (Zhang et al., 2023) and AiEdit datasets to establish unified comparative baselines. Furthermore, to investigate the impact of model scale and architectural differences on detection performance, we performed a systematic comparison among three base models, namely Qwen2.5-Omni-3B, Qwen2.5-Omni-7B, and Qwen2-Audio-7B, under identical experimental settings.

Regarding implementation details, all experiments were conducted on a single NVIDIA RTX 5880 GPU, and the training pipeline was implemented using the ms-swift framework. We applied full-parameter fine-tuning to the last three layers of the audio encoder and the projection layer, while the remaining modules were optimized via LoRA. The detailed hyperparameter configurations are provided in Appendix B.

In addition, the frame-level detector used to construct the word-level probabilistic prior is implemented based on the open-source BAM model (Zhong et al., 2024). This detector employs a WavLM-based feature extractor together with a frame-level prediction module to estimate the posterior probability of tampering for each frame. The training configuration strictly follows the official implementation, without introducing additional architectural modifications or hyperparameter tuning, thereby ensuring reproducibility and fairness of the experimental setup. Finally, the resulting frame-level probabilities are aggregated according to word boundary information (McAuliffe et al., 2017) to generate the acoustic prior incorporated into the proposed PELM framework.

5.2. Evaluation Metrics

We evaluate model performance at two granularities: (1) detection and (2) content localization. Specifically, the detection granularity assesses the model's ability to determine whether an entire audio clip contains edited content, while the content localization granularity measures the model's

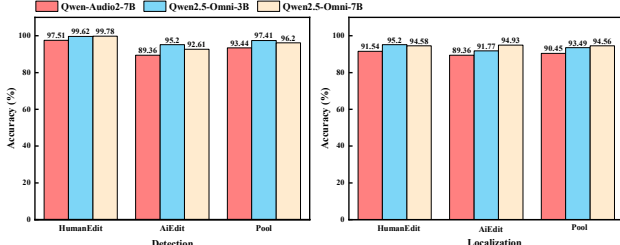


Figure 6. Performance evaluation of different models on speech editing tasks, including HumanEdit, AiEdit, and Pool. The left and right panels display the accuracy results under Detection and Localization level, respectively. Detailed results are provided in Appendix C.

capability to precisely identify the edited words within the utterance. The evaluation metrics include Accuracy, Area Under the Curve (AUC), F1 score, and Equal Error Rate (EER).

5.3. Comparative SOTA

To validate the effectiveness of the proposed method, we selected four state-of-the-art (SOTA) methods representing different technical paradigms as baselines for comparison: TDL (Xie et al., 2024) represents an efficient embedding-feature-based classification method; BAM (Zhong et al., 2024) represents a method utilizing explicit boundary attention mechanisms to enhance localization precision; AGO (Zeng et al., 2025) introduces gradient optimization and adversarial training strategies aimed at resolving multi-task conflicts and improving model generalization; and CF-PRF (Wu et al., 2024) represents a high-precision two-stage localization method incorporating a Proposal Regression paradigm.

The quantitative results in Table 2 reveal the limitations of existing methods when facing AI editing attacks, as well as the significant advantages of our method. On the HumanEdit dataset, the BAM model, based on boundary attention mechanisms, performs impressively and is on par with our method, indicating that traditional models can effectively capture acoustic traces left by manual splicing. However, on the more challenging AiEdit dataset, the performance of all baseline models drops precipitously; notably, TDL’s detection level F1 score plummets from 98.06% to 43.89%, suggesting that relying solely on acoustic features or boundary cues is insufficient to cope with highly smooth AI-generated forgeries. In contrast, the PELM method demonstrates superior robustness, maintaining an F1 score of 97.11% and a low EER of 8.37% on AiEdit.

5.4. Comparative baseline

The second part of the main experiment aims to conduct an in-depth analysis of the impact of different base models on performance. To this end, we select three representa-

Table 3. Ablation Study of Three dimensions. The ‘Train Param Ratio’ column indicates the percentage of trainable parameters relative to the full model. Reporting Acc. and EER (%) on HumanEdit and AiEdit.

Configuration	Train Param Ratio	HumanEdit				AiEdit												
		Detection		Localization		Detection		Localization										
Acc. ↑ EER ↓ Acc. ↑ EER ↓ Acc. ↑ EER ↓ Acc. ↑ EER ↓																		
Prompt Strategy: see Appendix D																		
Generic	-	99.4	0.56	93.61	0.7	91.48	12.49	90.1	13.3									
Descriptive	-	99.44	0.55	93.61	0.64	92.46	11.14	90.53	12.15									
Detailed	-	99.62	0.55	94.31	0.57	95.2	8.37	91.77	9.28									
LoRA Hyperparams																		
$r=16, \alpha=16$	-	98.96	0.62	94.34	0.62	91.21	13.76	90.55	13.76									
$r=16, \alpha=32$	-	98.94	0.55	94.41	0.55	94.17	11.42	90.89	11.42									
$r=32, \alpha=32$	-	98.88	0.59	94.41	0.59	94.13	12.14	91.05	12.14									
$r=32, \alpha=64$	-	99.62	0.55	94.31	0.57	95.2	8.37	91.77	9.28									
Fine-tuning Scope																		
Full-Depth LoRA	1.47%	99.02	0.56	93.94	0.56	94.35	10.11	91.17	10.11									
Audio Encoder	11.19%	99.04	0.55	94.54	0.57	94.34	10.11	91.13	10.82									
Last 3 Layers	2.27%	99.62	0.55	94.31	0.57	95.2	8.37	91.77	9.28									

tive models for comparative evaluation: Qwen2.5-Omni-3B, Qwen2.5-Omni-7B, and Qwen2.5-Audio-7B. Figure 6 provides a visual comparison of their accuracy across three evaluation granularities (the complete experimental results are reported in the Appendix). The results indicate that the Qwen2.5-Omni series significantly outperforms Qwen2.5-Audio in overall performance. This advantage primarily stems from its stronger pre-training generalization capability and superior multimodal instruction alignment, enabling the model to not only capture fine-grained acoustic cues but also more stably perform complex reasoning and structured text generation, thereby exhibiting enhanced comprehensive capability in detection and content localization tasks.

5.5. Ablation Study

To verify the efficacy of the design of each model component and explore the optimal configuration, we conducted comprehensive ablation studies across three dimensions: prompt design, LoRA hyperparameter sensitivity, and parameter fine-tuning scope. The experimental results are presented in Table 3.

Prompt strategy: First, regarding prompt design, considering that the level of detail in instructions directly impacts the reasoning and adherence capabilities of Large Language Models, we designed three prompt paradigms with a clear complexity gradient: (1) Generic brief instructions, where only the user prompt provides prior knowledge; (2) Definition-based instructions, which supplement the former with a clear definition of the task; and (3) Detailed instructions, which further introduce different editing operations and strict output format constraints (see Appendix for details). The experimental results reveal a significant instruction scaling trend: as the information density of instructions increases, the model’s discriminative ability steadily im-

Table 4. Ablation study on the effectiveness of key components. We report the Localization AUC (%) and EER (%) on HumanEdit and AiEdit datasets.

Prior Enhanced	Acoustic Constraint	HumanEdit		AiEdit	
		AUC↑	EER↓	AUC↑	EER↓
×	×	83.44	23.90	66.47	35.87
×	✓	88.56	18.77	66.87	35.80
✓	×	99.80	0.49	96.67	9.41
✓	✓	99.83	0.55	97.14	8.37
Frame Detector		99.21	3.78	92.89	15.89

proves. This indicates that introducing clear task definitions and reasoning steps can effectively reduce task ambiguity and guide the model to more precisely capture anomalous features in complex forgery scenarios.

LoRA hyperparameter: Second, regarding the hyperparameter configuration for LoRA fine-tuning, we focused on investigating the impact of the low-rank matrix dimension (Rank, r) and the scaling coefficient (Alpha, α). Here, r determines the capacity of trainable parameters and the upper limit of the model’s expressiveness, while α controls the magnitude of the adjustment (Scaling Factor) of new weights relative to pre-trained weights. To balance parameter efficiency and fitting capability, we conducted comparative experiments on four different sets of (r, α) combinations. The results indicate that a moderate increase in r can significantly enhance model capability.

Fine-tuning scope: Finally, we conducted an in-depth exploration of the fine-tuning scope. Given that the audio encoder of Qwen2.5-Omni contains 31 Transformer layers, we designed three different fine-tuning paradigms: (1) Full Depth LoRA: applying LoRA fine-tuning to all linear layers in the model, including both audio and text modules to test the most lightweight adaptation scheme; (2) High-level acoustic alignment: considering that the deep networks of the audio encoder often contain richer semantic information, we perform full parameter fine-tuning on the last three layers of the Audio Encoder and the projection layer, while using LoRA for the rest, aiming to strengthen the alignment between high-level acoustic features and text; and (3) Audio Encoder unfreezing: performing full parameter fine-tuning on the entire Audio Encoder to allow the audio feature extractor to undergo substantial adaptation, while the rest of the model remains under LoRA fine-tuning. As shown by the experimental results of the last configuration in Table 3, although performing full-parameter fine-tuning on the Audio Encoder can indeed unlock the model’s optimal performance potential, this comes with high computational costs. Specifically, this strategy causes the number of trainable parameters to surge to 11.19% of the total model parameters; under bf16 precision, merely maintaining the updates

of these parameters requires an additional 1.4GB of GPU memory. However, this significantly increased resource consumption did not yield a proportional performance leap. Considering the marginal effects of performance gains and resource constraints in practical deployment, we ultimately decided to only full parameters fine-tuning last 3 layers of audio encoder to seek the optimal balance between detection accuracy and computational efficiency.

Module Ablation: Table 4 evaluates the effectiveness of the prior-enhanced design and the acoustic consistency constraint in PELM. Without either component, localization performance drops sharply, indicating that semantic reasoning alone is insufficient for fine-grained speech editing detection. Introducing the word-level probabilistic prior leads to a decisive performance gain on both HumanEdit and AiEdit, substantially reducing EER. This confirms that explicit acoustic cues are critical for calibrating the reasoning boundaries of audio LLMs. The acoustic consistency constraint further improves robustness, yielding the best overall performance when combined with the prior. The frame-level detector can be regarded as the standalone performance of the prior itself. Although it provides reasonable localization capability, its lack of global contextual reasoning limits its effectiveness, highlighting the advantage of integrating prior knowledge with large-model inference in PELM.

6. Conclusion

To address the scarcity of high-quality data in speech editing detection and content localization tasks, this paper constructs the first large scale cross lingual benchmark dataset generated by integrating multiple advanced neural speech editing technologies. In this dataset, Large Language Models are employed to execute fine-grained semantic modifications covering addition, deletion, and modification operations, effectively filling the gap in high-fidelity AI-edited forgery data. Building upon this, we propose the Prior-Enhanced Audio LLM framework, PELM. By explicitly incorporating detection prior knowledge and an acoustic consistency aware loss, the framework effectively compels the large model to focus on the intrinsic differences of low-level acoustic signals during inference. This mechanism significantly mitigates the over-defensive bias and semantic drift problems potentially present in audio LLMs. Extensive experiments on both HumanEdit and AiEdit benchmarks demonstrate that PELM exhibits superior robustness and establishes new state-of-the-art performance records. Finally, in-depth ablation studies and configuration analyses validate the effectiveness of each core component, offering a research perspective for future efforts in utilizing large models to combat complex speech editing detection and achieve precise localization.

References

Playdiffusion. <https://github.com/playht/PlayDiffusion>.

Bai, H., Zheng, R., Chen, J., Ma, M., Li, X., and Huang, L. A³t: Alignment-aware acoustic and text pretraining for speech synthesis and editing. In *International Conference on Machine Learning*, pp. 1399–1411. PMLR, 2022.

Cai, Z., Stefanov, K., Dhall, A., and Hayat, M. Do you really mean that? content driven audio-visual deepfake dataset and multimodal method for temporal forgery localization. In *2022 International Conference on Digital Image Computing: Techniques and Applications (DICTA)*, pp. 1–10. IEEE, 2022.

Chen, Y., Niu, Z., Ma, Z., Deng, K., Wang, C., JianZhao, J., Yu, K., and Chen, X. F5-tts: A fairytaler that fakes fluent and faithful speech with flow matching. In *Proceedings of the 63rd Annual Meeting of the Association for Computational Linguistics (Volume 1: Long Papers)*, pp. 6255–6271, 2025.

Gu, H., Yi, J., Wang, C., Tao, J., Lian, Z., He, J., Ren, Y., Chen, Y., and Wen, Z. Allm4add: Unlocking the capabilities of audio large language models for audio deepfake detection. In *Proceedings of the 33rd ACM International Conference on Multimedia*, pp. 11736–11745, 2025.

Jiang, Z., Yang, Q., Zuo, J., Ye, Z., Huang, R., Ren, Y., and Zhao, Z. Fluentspeech: Stutter-oriented automatic speech editing with context-aware diffusion models. In *Findings of the Association for Computational Linguistics: ACL 2023*, pp. 11655–11671, 2023.

Kang, W., Yang, X., Yao, Z., Kuang, F., Yang, Y., Guo, L., Lin, L., and Povey, D. Libriheavy: A 50,000 hours asr corpus with punctuation casing and context. In *ICASSP 2024-2024 IEEE International Conference on Acoustics, Speech and Signal Processing (ICASSP)*, pp. 10991–10995. IEEE, 2024.

Koizumi, Y., Zen, H., Karita, S., Ding, Y., Yatabe, K., Morioka, N., Bacchiani, M., Zhang, Y., Han, W., and Bapna, A. Libritts-r: A restored multi-speaker text-to-speech corpus. In *Proc. Interspeech 2023*, pp. 5496–5500, 2023.

Luong, H.-T., Li, H., Zhang, L., Lee, K. A., and Chng, E. S. Llamapartialspoof: An llm-driven fake speech dataset simulating disinformation generation. In *ICASSP 2025-2025 IEEE International Conference on Acoustics, Speech and Signal Processing (ICASSP)*, pp. 1–5. IEEE, 2025.

Martín-Doñas, J. M. and Álvarez, A. The vicomtech audio deepfake detection system based on wav2vec2 for the 2022 add challenge. In *ICASSP 2022-2022 IEEE International Conference on Acoustics, Speech and Signal Processing (ICASSP)*, pp. 9241–9245. IEEE, 2022.

McAuliffe, M., Socolof, M., Mihuc, S., Wagner, M., and Sonderegger, M. Montreal forced aligner: Trainable text-speech alignment using kaldi. In *Interspeech*, volume 2017, pp. 498–502, 2017.

Peng, P., Huang, P.-Y., Li, S.-W., Mohamed, A., and Harwath, D. Voicecraft: Zero-shot speech editing and text-to-speech in the wild. In *Proceedings of the 62nd Annual Meeting of the Association for Computational Linguistics (Volume 1: Long Papers)*, pp. 12442–12462, 2024.

Röttger, P., Kirk, H., Vidgen, B., Attanasio, G., Bianchi, F., and Hovy, D. Xtest: A test suite for identifying exaggerated safety behaviours in large language models. In *Proceedings of the 2024 Conference of the North American Chapter of the Association for Computational Linguistics: Human Language Technologies (Volume 1: Long Papers)*, pp. 5377–5400, 2024.

Todisco, M., Wang, X., Vestman, V., Sahidullah, M., Delgado, H., Nautsch, A., Yamagishi, J., Evans, N., Kinunen, T. H., and Lee, K. A. Asvspoof 2019: Future horizons in spoofed and fake audio detection. *Interspeech 2019*, 2019.

Wang, H., Yu, M., Hai, J., Chen, C., Hu, Y., Chen, R., Dehak, N., and Yu, D. Ssr-speech: Towards stable, safe and robust zero-shot text-based speech editing and synthesis. In *ICASSP 2025-2025 IEEE International Conference on Acoustics, Speech and Signal Processing (ICASSP)*, pp. 1–5. IEEE, 2025a.

Wang, J., Ma, Z., Luo, Z., Wang, T., Ge, M., Wang, X., and Wang, L. Pay more attention to audio: Mitigating imbalance of cross-modal attention in large audio language models. *arXiv preprint arXiv:2509.18816*, 2025b.

Wu, J., Lu, W., Luo, X., Yang, R., Wang, Q., and Cao, X. Coarse-to-fine proposal refinement framework for audio temporal forgery detection and localization. In *Proceedings of the 32nd ACM International Conference on Multimedia*, pp. 7395–7403. ACM, October 2024.

Xie, Y., Cheng, H., Wang, Y., and Ye, L. An efficient temporary deepfake location approach based embeddings for partially spoofed audio detection. In *ICASSP 2024-2024 IEEE International Conference on Acoustics, Speech and Signal Processing (ICASSP)*, pp. 966–970. IEEE, 2024.

Yamagishi, J., Veaux, C., and MacDonald, K. Cstr vctk corpus: English multi-speaker corpus for cstr voice cloning toolkit (version 0.92). *The Rainbow Passage*

which the speakers read out can be found in the International Dialects of English Archive:(<http://web.ku.edu/~idea/readings/rainbow.htm>)., 2019.

Yamagishi, J., Wang, X., Todisco, M., Sahidullah, M., Patino, J., Nautsch, A., Liu, X., Lee, K. A., Kinnunen, T., Evans, N., et al. Asvspoof 2021: accelerating progress in spoofed and deepfake speech detection. In *Proc. ASVspoof 2021*, pp. 47–54, 2021.

Yan, C., Jin, C., Huang, D., Yu, H., Peng, H., Zhan, H., Gao, J., Peng, J., Chen, J., Zhou, J., et al. Ming-uniaudio: Speech llm for joint understanding, generation and editing with unified representation. *arXiv preprint arXiv:2511.05516*, 2025.

Yao, J., Yuguang, Y., Pan, Y., Ning, Z., Ye, J., Zhou, H., and Xie, L. Stablevc: Style controllable zero-shot voice conversion with conditional flow matching. In *Proceedings of the AAAI Conference on Artificial Intelligence*, volume 39, pp. 25669–25677, 2025.

Yi, J., Bai, Y., Tao, J., Ma, H., Tian, Z., Wang, C., Wang, T., and Fu, R. Half-truth: A partially fake audio detection dataset. In *Proc. Interspeech 2021*, pp. 1654–1658, 2021.

Yi, J., Fu, R., Tao, J., Nie, S., Ma, H., Wang, C., Wang, T., Tian, Z., Bai, Y., Fan, C., et al. Add 2022: the first audio deep synthesis detection challenge. In *ICASSP 2022-2022 IEEE International Conference on Acoustics, Speech and Signal Processing (ICASSP)*, pp. 9216–9220. IEEE, 2022.

Yi, J., Tao, J., Fu, R., Yan, X., Wang, C., Wang, T., Zhang, C. Y., Zhang, X., Zhao, Y., Ren, Y., Xu, L., Zhou, J., Gu, H., Wen, Z., Liang, S., Lian, Z., Nie, S., and Li, H. Add 2023: the second audio deepfake detection challenge, 2023a.

Yi, J., Tao, J., Fu, R., Yan, X., Wang, C., Wang, T., Zhang, C. Y., Zhang, X., Zhao, Y., Ren, Y., et al. Add 2023: the second audio deepfake detection challenge. *arXiv preprint arXiv:2305.13774*, 2023b.

Zeng, S., Yi, J., Tao, J., He, J., Lian, Z., Liang, S., Zhang, C., Chen, Y., and Zhang, X. Adversarial training and gradient optimization for partially deepfake audio localization. In *ICASSP 2025-2025 IEEE International Conference on Acoustics, Speech and Signal Processing (ICASSP)*, pp. 1–5. IEEE, 2025.

Zhang, B. and Sim, T. Localizing fake segments in speech. In *2022 26th International Conference on Pattern Recognition (ICPR)*, pp. 3224–3230. IEEE, 2022.

Zhang, L., Wang, X., Cooper, E., Evans, N., and Yamagishi, J. The partialspoof database and countermeasures for the detection of short fake speech segments embedded in an utterance. *IEEE/ACM Transactions on Audio, Speech, and Language Processing*, 31:813–825, 2023. ISSN 2329-9304.

Zhang, Y., Tian, B., Zhang, L., and Duan, Z. PartialEdit: Identifying Partial Deepfakes in the Era of Neural Speech Editing . In *Interspeech 2025*, pp. 5353–5357, 2025.

Zhao, J., Jia, Y., Wang, S., Zhou, J., Wang, H., and Qin, Y. Chinese-lips: A chinese audio-visual speech recognition dataset with lip-reading and presentation slides. In *2025 IEEE International Conference on Multimedia and Expo (ICME)*, pp. 1–6. IEEE, 2025.

Zhong, J., Li, B., and Yi, J. Enhancing partially spoofed audio localization with boundary-aware attention mechanism. In *Proc. Interspeech 2024*, pp. 4838–4842, 2024.

A. Dataset Construction and Statistics

A.1. Dataset Construction Specifications and Format

To ensure the precision and atomic nature of the parallel corpus, we strictly define three types of editing operations: Add, Delete, and Modify. As detailed in Table 5, each operation is subject to rigorous constraints to maintain context integrity. For instance, the Delete operation strictly prohibits removing words at sentence boundaries, and all operations are restricted to a single continuous region per sample to avoid ambiguity.

Table 5. Definitions and strict constraints for atomic editing operations employed in data construction.

Operation	Definition	Strict Constraints
Add	Inserts new semantically relevant content into the original text.	1. Must originate from the original context. 2. Only <i>one</i> continuous insertion point is allowed per sample.
Delete	Removes a segment of text from the original sentence.	1. Removal of words at the start or end of the sentence is strictly prohibited to preserve context integrity. 2. Only <i>one</i> continuous deletion region is allowed.
Modify	Replaces a segment of the original text with new content.	1. The replacement must maintain a similar length to the original segment. 2. Only <i>one</i> modification region is allowed (i.e., one replacement).

Finally, to ensure reproducibility, the detailed hyperparameters and environmental settings used for the parallel text editing tool are listed in Table 6.

Table 6. Hyperparameters and settings for the Qwen-based parallel text editing tool.

Parameter	Value	Description
Model Name	Qwen3-max	The backbone LLM used for text generation.
Max Workers	20	Number of concurrent threads for parallel processing.
Batch Size	50	Number of samples processed in a single internal batch.
Max Retries	5	Maximum attempts for the LLM to regenerate if validation fails.
Diff Engine	difflib	Python library used for calculating precise word-level differences.
Validation	Double	Two-stage verification enabled for strict quality control.

To ensure the high quality and structural integrity of the constructed parallel corpus, we implemented a rigorous three-stage Quality Assurance (QA) pipeline.

The process begins with a **Strict Validation** phase immediately following the LLM generation. By utilizing the Python `difflib` library, we calculate precise word-level differences between the source and target texts. This step verifies that the generated edit strictly adheres to the topological constraints defined in Table 5, such as ensuring no deletions occur at sentence boundaries and that modifications are confined to a single continuous region.

Subsequently, if a sample fails this initial validation, an **Automatic Retry** mechanism is triggered. The system prompts the model to regenerate the response, allowing for a maximum of 5 attempts to correct the logical violation.

Finally, in scenarios where the model fails to produce a valid output after all retries, a **Heuristic Fallback** algorithm is employed. This rule-based mechanism generates a synthetic edit to preserve the data entry structure but explicitly flags the sample by setting `IS_AVAILABLE=False`, thereby enabling easy filtration of low-quality data during downstream training phases.

A.2. Dataset Statistics

Table 7 details the sample distribution across the training, validation, and test sets, categorized into ADD, DELETE, MODIFY, and Real types. The statistics indicate that the test set comprises the largest volume (45,970 samples), and the MODIFY category consistently accounts for the highest proportion across all subsets, highlighting its dominance in the dataset composition.

Table 7. Statistics of sample quantities across different dataset splits and operation types

	Total	ADD	DELETE	MODIFY	Real
Train	11328	1753	2790	4792	1993
Val	2256	357	561	941	397
Test	45970	8411	13206	18983	5370
Total	59554	10521	16557	24716	7760

Table 8 lists the neural editing models employed in the training, validation, and test sets. Here, 'Ming' and 'SSR' refer to Ming-UniAudio and SSR-Speech, respectively. Regarding nomenclature, the suffixes '.CN' and '.EN' denote Chinese and English datasets, respectively, while models without suffixes are English by default. Additionally, FluentSpeech is categorized into two variants based on its pre-training data, VCTK (Yamagishi et al., 2019) and Libritts (Koizumi et al., 2023).

Table 8. List of neural editing models employed across different dataset splits.

Split	Neural Editing Models
Train	FluentSpeech, Ming.CN, Ming.EN, PlayDiffusion, VoiceCraft
Val	FluentSpeech, Ming.CN, Ming.EN, PlayDiffusion, VoiceCraft
Test	A3T, SSR.CN, SSR.EN, FluentSpeech, Ming.CN, Ming.EN, PlayDiffusion, VoiceCraft

To facilitate reproducibility and further research, Table 9 provides the official open-source implementations for all baseline neural editing models employed in our experiments.

Table 9. Official code repositories for the neural editing models utilized in this study.

Editing Model	Ref.	Official Repository
A3T	(Bai et al., 2022)	https://github.com/richardbaihe/a3t
FluentSpeech	(Jiang et al., 2023)	https://github.com/Zain-Jiang/Speech-Editing-Toolkit
Ming-UniAudio	(Yan et al., 2025)	https://github.com/inclusionAI/Ming-UniAudio
PlayDiffusion	(pla)	https://github.com/playht/PlayDiffusion
SSR-Speech	(Wang et al., 2025a)	https://github.com/WangHelin1997/SSR-Speech
VoiceCraft	(Peng et al., 2024)	https://github.com/jasonppy/VoiceCraft

B. Detailed Model Structure

Unless otherwise specified, all fine-tuning experiments are conducted using the Qwen-2.5-Omni-3B model. We fine-tune the Qwen-2.5-Omni-3B model using the AdamW optimizer with a peak learning rate of 1×10^{-5} and a cosine learning rate scheduler. To ensure training stability, we apply a warmup ratio of 0.2 and a weight decay of 0.1. The training is conducted for 5 epochs with a global batch size of 8 and a maximum sequence length of 2048. For parameter-efficient fine-tuning via LoRA, we set the rank $r = 32$, scaling factor $\alpha = 64$, and dropout rate to 0.05. We set the weight λ for the acoustic consistency constraint to 0.5, ensuring that the top- k proportion is kept at a distance beyond the centroid margin. Detailed hyperparameter settings are listed in Table 10.

Table 10. Hyperparameter settings for fine-tuning the Default model.

Hyperparameters	Value
Base Model	Qwen-2.5-Omni-3B
Training Epochs	5
Global Batch Size	8
Max Sequence Length	2048
Optimizer	AdamW
Learning Rate	1×10^{-5}
LR Scheduler	Cosine
Warmup Ratio	0.2
Weight Decay	0.1
LoRA Rank (r)	32
LoRA Alpha (α)	64
LoRA Dropout	0.05
λ	0.5
margin	0.9
topk	0.1

C. Complete Results.

C.1. Comparison of different base model

Table 11 presents a comprehensive comparison of different base models. The results demonstrate that the Qwen2.5-Omni series significantly outperforms the Qwen2-Audio baseline across both benchmarks. Notably, despite its smaller size, Qwen2.5-Omni-3B achieves the best overall performance, particularly excelling in the challenging Correction task and the AiEdit benchmark.

Table 11. Complete Performance Evaluation of Different Base Models on HumanEdit and AiEdit Benchmarks at Multiple Granularities.

Model	HumanEdit						AiEdit					
	Detection			Localization			Detection			Localization		
	Acc. \uparrow	AUC \uparrow	F1 \uparrow	EER \downarrow	Acc. \uparrow	AUC \uparrow	F1 \uparrow	EER \downarrow	Acc. \uparrow	AUC \uparrow	F1 \uparrow	EER \downarrow
Qwen2-Audio-7B	97.51	99.45	98.53	0.74	91.54	99.45	99.76	0.74	89.36	59.27	94.24	44.88
Qwen2.5-Omni-3B	99.62	99.83	99.78	0.55	94.31	99.80	99.70	0.57	95.20	97.14	97.29	8.37
Qwen2.5-Omni-7B	99.76	99.85	99.86	0.64	94.10	99.85	99.84	0.64	95.29	95.36	97.37	11.03
												87.82
												95.36
												97.36
												11.03

D. Training Prompt

We designed three distinct prompt strategies ranging from simple to complex. Figure 7 represents the simplest baseline; it utilizes a default system prompt and provides context information solely within the user prompt. Figure 8 represents an intermediate strategy that incorporates a specific task definition and simple output instructions into the system prompt, explicitly guiding the model to perform speech editing detection. Finally, Figure 9 illustrates the most comprehensive design, which enforces strict output formatting constraints and detailed editing type classifications to ensure precise and standardized generation.

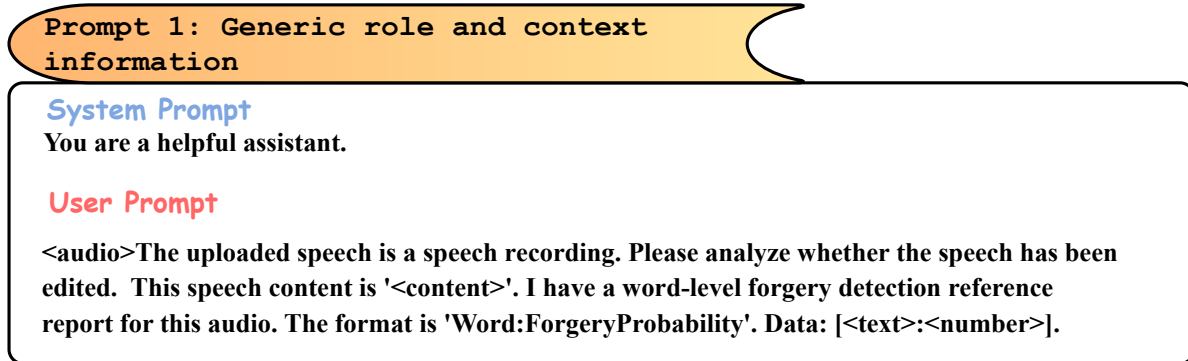


Figure 7. Prompt details of generic prompt

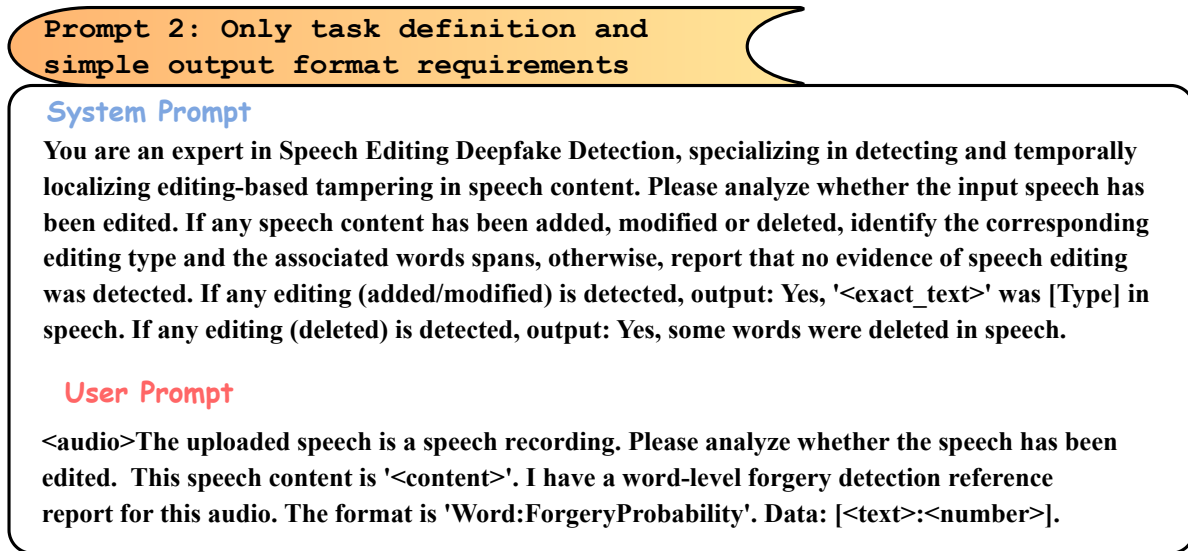


Figure 8. Prompt details of task definition only prompt

Prompt 3: Complete task definition and strict output format requirements

System Prompt

You are an expert in Speech Editing Deepfake Detection, specializing in detecting and temporally localizing editing-based tampering in speech content. Please analyze whether the input speech has been edited. If any speech content has been added, modified or deleted, identify the corresponding editing type and the associated words spans, otherwise, report that no evidence of speech editing was detected.

Output Requirements:

1. If the speech is completely authentic, output: "No evidence of speech editing was detected."
2. If any editing (added/modified/deleted) is detected, output:
 - 1) If the editing is added or modified, output: "Yes, '<exact_text>' was [Type] in speech. The [Type] MUST be one of the following: added, modified."
 - 2) If the editing is deleted, output: "Yes, some words were deleted in speech."
3. Treat every speech fairly.
4. Do not output any other text or explanation. Output ONLY the result string.

Output Examples:

No evidence of speech editing was detected.

Yes, '不' was added in speech.

Yes, 'dull' was modified in speech.

Yes, some words were deleted in speech.

User Prompt

<audio>The uploaded speech is a speech recording. Please analyze whether the speech has been edited. If any speech content has been added, deleted, or modified, identify the corresponding editing type and the associated words; otherwise, report that no evidence of speech editing was detected. This speech content is '<content>'. I have a word-level forgery detection reference report for this audio. The format is 'Word:ForgeryProbability'. Data: [<text>:<number>]. Treat this report with caution as it is not a definitive answer.

Figure 9. Prompt details of complete task definition with strict requirements